Roles of Thermal and Radical Quenching in Emissions of Wall-Stabilized Hydrogen Flames

P. Aghalayam and D. G. Vlachos
Dept. of Chemical Engineering, University of Massachusetts Amherst, Amherst, MA 01003

A numerical study of the combustion of H_2/air mixtures impinging on surfaces has been performed, using detailed chemistry and multicomponent transport, in order to elucidate the roles of surface thermal and chemical quenching in pollutant emissions. For extinguishable fuel/air mixtures, the thermal coupling with the surface has been found to be strong, and surface thermal quenching reduces NO_x emissions. However, nonextinguishable mixtures are practically unaffected by changes in surface temperature, except for an increase in NO_2 at low surface temperatures. It is shown that radical wall quenching can affect emissions for all flames, with H being the most important one primarily for NO_2 near the surface, due to the reaction $NO_2 + H \leftrightarrow NO + OH$. A new method to elucidate the dominant paths for NO formation is also presented.

Introduction

In recent years, the study of NO_x emissions has gained importance, due to the stringent environmental regulations. The interaction between combustible gases and surfaces is important in determining emissions from a system. Excess emissions of unburned hydrocarbons in combustion engines have long been attributed to the presence of cool walls (Daniel, 1956; Westbrook et al., 1981; Kiehne et al., 1986; Hocks et al., 1981; Sloane and Schoene, 1983). In a related problem, the conversion of NO to NO_2 when a combusted gas comes in contact with the wall of water-cooled measurement probes has evoked some interest and speculation about the accuracy of NO_x measurements (Hori, 1986). Over the last decade, the interaction between hot combustion products with cool air encountered in turbulent diffusion flames has been studied experimentally and numerically, showing also an increased conversion of NO to NO_2 (Sano, 1984, 1985; Hori, 1988; Hori et al., 1992). In radiant surface burners, the thermal coupling between the surface and the flame has been found experimentally to lead to lower NO_x (Williams et al., 1992). The above problems indicate that gaining deeper insight into the physics controlling emissions related to flame-surface interactions is important, but is currently lacking.

Here, we analyze an H_2/air mixture impinging onto a wall of controlled temperature at steady state (a surface-stabilized flame) using detailed gas-phase chemistry and multicomponent transport. The effects of thermal interactions through heat loss and chemical interactions through radical quenching between a flame and a surface on emissions are studied for the first time using continuation techniques at different conditions of operation, and are analyzed using rates and reaction path analysis across the flame. The importance of various pathways to NO_x formation, including the thermal, NNH, and N_2O mechanisms at various conditions, is also discussed.

Model

A stagnation-point flow geometry is modeled, where a premixed fuel-air mixture impinges onto a flat wall surface. The partial differential equations of continuity, momentum, species, and energy are converted to ordinary differential equations (ODEs) using a similarity transformation. A second-order finite difference scheme is used to discretize the ODEs on a uniform mesh of 251 nodes. The resulting set of nonlinear algebraic equations (about 5,000 in number) is solved using Newton's technique. The differential equations are listed elsewhere (Bui et al., 1997). The mass and energy boundary conditions are listed in Table 1.

The $H_2 - NO_x$ submechanism of the GRI 2.11 methane mechanism is employed (Bowman et al., 1995), shown in Table 2, and consists of 18 reactive species among 70 reversible reactions. Its associated thermodynamic database is used to compute the heats of reactions and the equilibrium constants. Mixture average diffusivities are calculated using the

Correspondence concerning this article should be addressed to D. G. Vlachos.

Table 1. Mass and Energy Boundary Conditions

Quantity	Ambient	Wall
Energy	$T = T_e$	$k\left(\frac{\partial T}{\partial y}\right)_{y=0} - \sum_{i=1}^{N_s} r_i^s \Delta H_i^s + P_w = 0$
Gas Species	$W_j = W_{ej}$	$-\frac{D_j \rho}{M}\left(\frac{(\partial W_j \bar{M})}{\partial y}\right)_{y=0} = \sum_{i=1}^{N_s} \nu_{ij} r_i^s M_j,\ j = 1,2,\ldots,m_g$
Carrier Species		$W_{\text{carrier}} = 1 - \sum_{j=1}^{m_g} W_i$
Surface Species		$0 = \sum_{i=1}^{N_s} \nu_{ij} r_i^s,\ j = 1,2,\ldots,m_s,\ j \neq \bigstar$
Vacancies		$\theta_\bigstar = 1 - \sum_{j=1}^{m_s} \theta_j,\ j \neq \bigstar$

CHEMKIN database (Kee et al., 1990). The GRI mechanism has been extensively validated against experimental data giving good agreement.

The conditions for most simulations are a strain rate (hydrodynamic velocity gradient) of 1,000 s^{-1}, a pressure of 1 atm, and an inlet temperature of 25°C, unless otherwise stated. Combustion near an inert surface is first discussed. The roles of strain rate and radical wall recombination are discussed at the end of the article.

Ignition, Extinction, and Autothermal Behavior

A brief overview is given on the important bifurcation characteristics of fuel-lean H_2/air flames, as related to emissions. More details of the bifurcation behavior of flames near inert and catalytic surfaces for H_2/air and CH_4/air flames can be found in Vlachos et al. (1993, 1994, 1997), Vlachos (1995), and Bui et al. (1997).

Figure 1a shows the surface temperature vs. the power supply to the surface for three inlet compositions: 10% (dotted lines), 16% (dashed lines), and 28% H_2/air (solid lines). For sufficiently fuel-lean mixtures, such as 10% inlet H_2 in air, as the power supplied to the surface increases from low values, there is an increase in surface temperature up to the ignition point. A slight further increase in the power results in an abrupt jump from the extinguished to the ignited branch with a considerable increase in surface temperature. Conversely, when the power supply is reduced down from high values along the ignited branch, there is a discontinuous transition from the ignited to the extinguished branch at extinction. The high temperatures observed near the surface are lower in practical systems due to surface heat loss (such as by radiation) and serve here only as a limited upper bound. The effect of thermal quenching will be discussed in the following section.

As the inlet composition is increased, the extinction temperature decreases sharply. As an example, for intermediate compositions such as 16% H_2 in air, extinction would occur experimentally at a surface temperature of ~ 350 K. For mixtures close to the stoichiometric point such as 28% inlet H_2, ignition leads to a fully ignited branch (AB), which is in fact disjoined from the rest of the branches (an isolated branch). Upon surface thermal quenching, no flame extinction occurs. This gas mixture is said to be nonextinguishable. For these conditions, the fuel-lean extinguishable limit is found to be at about 16% inlet H_2 in air.

For a self-sustained flame, that is, when the power input to the system is zero, the operation is called *adiabatic* (in the absence of heat loss). For example, in Figure 1a, A and C are the higher-temperature adiabatic operation points for 28% and 10% inlet H_2/air mixtures, respectively. The temperature window for energy production is bounded by the higher adiabatic temperature and extinction (where it exists).

Figure 1b shows the adiabatic surface temperature and the corresponding mole fractions of H_2 and NO_x species adjacent to the surface as a function of inlet composition for fuel-lean mixtures, which are of interest in energy production. It is observed that the surface temperature is higher for mixtures near the stoichiometric point and decreases, as expected, with a decrease in inlet composition. Below an inlet composition of $\sim 8\%$ H_2 in air (*fuel-lean adiabatic point*), there is no more adiabatic operation because, for these very fuel-lean mixtures, the heat generated from the system is not sufficient to sustain combustion. The locus of extinction temperatures is also indicated in this plot.

As the inlet fuel composition decreases from the stoichiometric one, the H_2 mole fraction first decreases, goes through a minimum at about 17% inlet H_2/air, and then increases again for fuel-leaner compositions. NO is present in high levels (up to ~ 250 ppm), and is maximum near the stoichiometric point. As the inlet H_2 composition decreases, a significant drop in NO is observed, especially near the fuel-lean adiabatic point (to levels below ~ 1 ppm). N_2O is relatively unaffected by changes in inlet composition, and NO_2 exhibits similar trends as NO. Furthermore, N_2O and NO_2 are well below 1 ppm at all compositions. Our simulations indicate that *while fuel-lean mixtures exhibit low temperature and NO_x mole fractions, they result in high fuel emissions*. Thus, there is a trade-off between fuel and NO_x emissions.

Role of Thermal Quenching in Emissions

The temperature of the surface can decrease due to various heat loss mechanisms (such as radiation, conduction, and convection at the back of the surface). In addition, the stagnation surface can be used as a heat exchanger, where energy is extracted by a fluid contacting the back of the surface (*an integrated reactor/heat exchanger unit*).

Table 2. Gas-Phase Reaction Mechanism

No.	Reactions	k_o	β	E (cal/mol)	No.	Reactions	k_o	β	E (cal/mol)
1_a	$2O+M \leftrightarrow O_2+M$	1.20e+17	−1.00	0.0	36	$NO_2+H \leftrightarrow NO+OH$	1.32e+14	0.00	360.0
2_b	$H+O+M \leftrightarrow OH+M$	5.00e+17	−1.00	0.0	37	$NH+O \leftrightarrow NO+H$	5.00e+13	0.00	0.0
3	$H_2+O \leftrightarrow H+OH$	5.00e+4	2.67	6,290.0	38	$NH+H \leftrightarrow N+H_2$	3.20e+13	0.00	330.0
4	$O+HO_2 \leftrightarrow O_2+OH$	2.00e+13	0.00	0.0	39	$NH+OH \leftrightarrow HNO+H$	2.00e+13	0.00	0.0
5	$O+H_2O_2 \leftrightarrow OH+HO_2$	9.63e+6	2.00	4,000.0	40	$NH+OH \leftrightarrow N+H_2O$	2.00e+9	1.20	0.0
6_c	$H+O_2+M \leftrightarrow HO_2+M$	2.80e+18	−0.86	0.0	41	$NH+O_2 \leftrightarrow HNO+O$	4.61e+5	2.00	6,500.0
7_d	$H+O_2+M \leftrightarrow HO_2+M$	3.00e+20	−1.72	0.0	42	$NH+O_2 \leftrightarrow NO+OH$	1.28e+6	1.50	100.0
8_e	$H+O_2+M \leftrightarrow HO_2+M$	9.38e+18	−0.76	0.0	43	$NH+H_2O \leftrightarrow HNO+H_2$	2.00e+13	0.00	13,850.0
9_f	$H+O_2+M \leftrightarrow HO_2+M$	3.75e+20	−1.72	0.0	44	$NH+NO \leftrightarrow N_2O+H$	4.16e+14	−0.45	0.0
10	$H+O_2 \leftrightarrow HO_2$	7.00e+17	−0.80	0.0	45	$NH_2+O \leftrightarrow OH+NH$	7.00e+12	0.00	0.0
11	$H+O_2 \leftrightarrow O+OH$	8.30e+13	0.00	14,413.0	46	$NH_2+O \leftrightarrow H+HNO$	4.60e+13	0.00	0.0
12_g	$2H+M \leftrightarrow H_2+M$	1.00e+18	−1.00	0.0	47	$NH_2+H \leftrightarrow NH+H_2$	4.00e+13	0.00	3,650.0
13_h	$2H+M \leftrightarrow H_2+M$	9.00e+16	−0.60	0.0	48	$NH_2+OH \leftrightarrow NH+H_2O$	9.00e+7	1.50	−460.0
14_i	$2H+M \leftrightarrow H_2+M$	6.00e+19	−1.25	0.0	49	$NNH+O \leftrightarrow NH+NO$	7.00e+13	0.00	0.0
15	$2H \leftrightarrow H_2$	5.50e+20	−2.00	0.0	50_m	$H+NO+M \leftrightarrow HNO+M$	8.95e+19	−1.32	740.0
16_j	$H+OH+M \leftrightarrow H_2O+M$	2.20e+22	−2.00	0.0	51	$HNO+O \leftrightarrow NO+OH$	2.50e+13	0.00	0.0
17	$H+HO_2 \leftrightarrow O+H_2O$	3.97e+12	0.00	671.0	52	$HNO+H \leftrightarrow H_2+NO$	4.50e+11	0.72	660.0
18	$H+HO_2 \leftrightarrow H_2+O_2$	2.80e+13	0.00	1,068.0	53	$HNO+OH \leftrightarrow NO+H_2O$	1.30e+7	1.90	−950.0
19	$H+HO_2 \leftrightarrow 2OH$	1.34e+14	0.00	635.0	54	$HNO+O_2 \leftrightarrow HO_2+NO$	1.00e+13	0.00	13,000.0
20	$H+H_2O_2 \leftrightarrow H_2+HO_2$	1.21e+7	2.00	5,200.0	55	$NH_3+H \leftrightarrow NH_2+H_2$	5.40e+5	2.40	9,915.0
21	$H+H_2O_2 \leftrightarrow OH+H_2O$	1.00e+13	0.00	3,600.0	56	$NH_3+OH \leftrightarrow NH_2+H_2O$	5.00e+7	1.60	955.0
22	$H_2+OH \leftrightarrow H+H_2O$	2.16e+8	1.51	3,430.0	57	$NH_3+O \leftrightarrow NH_2+OH$	9.40e+6	1.94	6,460.0
23_k	$2OH+M \leftrightarrow H_2O_2+M$	7.40e+13	−0.37	0.0	58	$N+NO \leftrightarrow N_2+O$	3.50e+13	0.00	330.0
	TROE	2.30e+18	−0.90	−1,700.0	59	$N_2O+O \leftrightarrow N_2+O_2$	1.40e+12	0.00	10,810.0
		0.7346 94.00 1756.0		5,182.0	60	$N_2O+H \leftrightarrow N_2+OH$	4.40e+14	0.00	18,880.0
24	$2OH \leftrightarrow O+H_2O$	3.57e+4	2.40	−2,110.0	61	$N_2O+OH \leftrightarrow N_2+HO_2$	2.00e+12	0.00	21,060.0
25	$OH+HO_2 \leftrightarrow O_2+H_2O$	2.90e+13	0.00	−500.0	62_n	$N_2O+M \leftrightarrow N_2+O+M$	1.30e+11	0.00	59,620.0
26	$OH+H_2O_2 \leftrightarrow HO_2+H_2O$	1.75e+12	0.00	320.0		LINDEMANN	6.20e+14	0.00	56,100.0
27	$OH+H_2O_2 \leftrightarrow HO_2+H_2O$	5.80e+14	0.00	9,560.0	63	$NH+N \leftrightarrow N_2+H$	1.50e+13	0.00	0.0
28	$2HO_2 \leftrightarrow O_2+H_2O_2$	1.30e+11	0.00	−1,630.0	64	$NH+NO \leftrightarrow N_2+OH$	2.16e+13	−0.23	0.0
29	$2HO_2 \leftrightarrow O_2+H_2O_2$	4.20e+14	0.00	12,000.0	65	$NNH \leftrightarrow N_2+H$	3.30e+08	0.00	0.0
30	$N+O_2 \leftrightarrow NO+O$	2.65e+12	0.00	6,400.0	66_o	$NNH+M \leftrightarrow N_2+H+M$	1.30e+14	−0.11	4,980.0
31	$N+OH \leftrightarrow NO+H$	7.33e+13	0.00	1,120.0	67	$NNH+O_2 \leftrightarrow HO_2+N_2$	5.00e+12	0.00	0.0
32	$N_2O+O \leftrightarrow 2NO$	2.90e+13	0.00	23,150.0	68	$NNH+O \leftrightarrow OH+N_2$	2.50e+13	0.00	0.0
33	$HO_2+NO \leftrightarrow NO_2+OH$	2.11e+12	0.00	−480.0	69	$NNH+H \leftrightarrow H_2+N_2$	5.00e+13	0.00	0.0
34_l	$NO+O+M \leftrightarrow NO_2+M$	1.06e+20	−1.41	0.0	70	$NNH+OH \leftrightarrow H_2O+N_2$	2.00e+13	0.00	0.0
35	$NO_2+O \leftrightarrow NO+O_2$	3.90e+12	0.00	−240.0					

The units of k_0 are in moles, cubic centimeters, and seconds. The reaction rate constant is computed using the modified Arrhenius expression $k_0 T^{\beta} e^{-E/RT}$. *a*: $\omega_1(H_2)=2.40$, $\omega_1(H_2O)=15.4$; *b*: $\omega_2(H_2)=2.0$, $\omega_2(H_2)=6.0$; *c*: $\omega_6(O_2)=0.0$, $\omega_6(H_2)=0.0$; *d*: $\omega_7(O_2)=1.0$; *e*: $\omega_8(H_2O)=1.0$; *f*: $\omega_9(N_2)=1.0$; *g*: $\omega_{12}(H_2)=0.0$, $\omega_{12}(H_2O)=0.0$; *h*: $\omega_{13}(H_2)=1.0$; *i*: $\omega_{14}(H_2O)=1.0$; *j*: $\omega_{16}(H_2)=0.73$, $\omega_{16}(H_2O)=3.65$; *k*: $\omega_{23}(H_2)=2.0$, $\omega_{23}(H_2O)=6.0$; *l*: $\omega_{34}(H_2)=2.0$, $\omega_{34}(H_2O)=6.0$; *m*: $\omega_{50}(H_2)=2.0$, $\omega_{50}(H_2O)=6.0$; *n*: $\omega_{62}(H_2)=2.0$; $\omega_{62}(H_2O)=6.0$; *o*: $\omega_{66}(H_2)=2.0$, $\omega_{66}(H_2O)=6.0$.

In order to study the effect of surface thermal quenching, simulations were performed, wherein cuts shown as vertical arrows in Figure 1b were followed, that is, at a fixed inlet composition, the surface temperature was reduced down from the adiabatic one. The 28% and 10% inlet H_2/air mixtures were considered, as representative of nonextinguishable and extinguishable self-sustained flames, respectively, according to Figure 1a.

Nonextinguishable flames

Figure 2 shows the flame structure (profiles) for 28% inlet H_2/air, that is, the temperature and mole fractions of various species as a function of the distance from the surface at surface temperatures represented by points *A* (adiabatic operation) and *B* (quenched flame) in Figure 1a. It is observed that such nonextinguishable mixtures burn vigorously away from the wall (a thick boundary layer), and exhibit high temperatures throughout the boundary layer at adiabatic conditions. The mole fractions of species remain almost constant across the whole boundary layer showing an abrupt combustion front at a distance of about 0.5 cm from the surface. This indicates a transition from a reaction zone, where the reactants are consumed at a very high rate, to a post-combustion zone, where the oxidation is slower.

When the surface temperature is reduced, the boundary layer shrinks slightly, and the mole fraction of H_2 decreases slightly in a small sublayer of the boundary layer, called the frozen sublayer. Thermal quenching considerably reduces the mole fractions of H and O and increases the mole fraction of HO_2 near the surface. The latter is due to the fact that low temperatures favor the production of HO_2 through the reaction $H+O_2+M \rightarrow HO_2+M$, which is nonactivated (see Table 2). Since the concentration of radicals remains high in the bulk of the boundary layer, extinction is not possible, despite very low surface temperatures. Thus, under these conditions, the thermal coupling between the surface and the flame is not strong enough to affect flame stability (a low heat-transfer coefficient between the reaction zone and the surface). The surface then acts more like a flame holder.

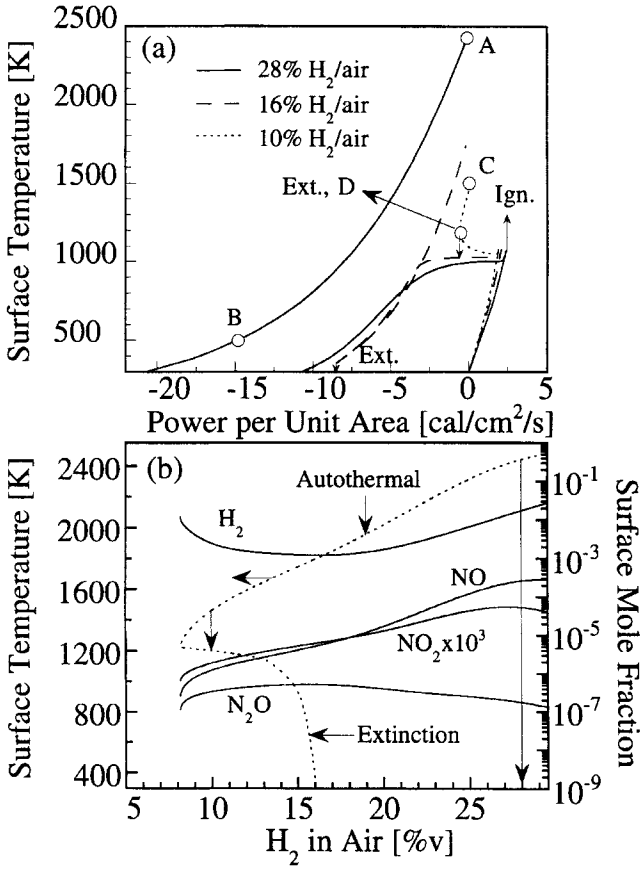

Figure 1. Surface temperature vs. power supplied to the surface for selected compositions (panel a).

The near-stoichiometric mixture is nonextinguishable, and the ignited branch (AB) is disjoined from the rest of the branches. Surface temperature and surface mole fractions of H_2 and NO_x, as a function of the inlet fuel composition, along the autotherm are shown in panel b. The extinction temperatures are also indicated. The NO and NO_2 mole fractions decrease with a drop in inlet composition. The conditions are pressure of 1 atm, strain rate of 1,000 s^{-1}, and inlet temperature of 25°C.

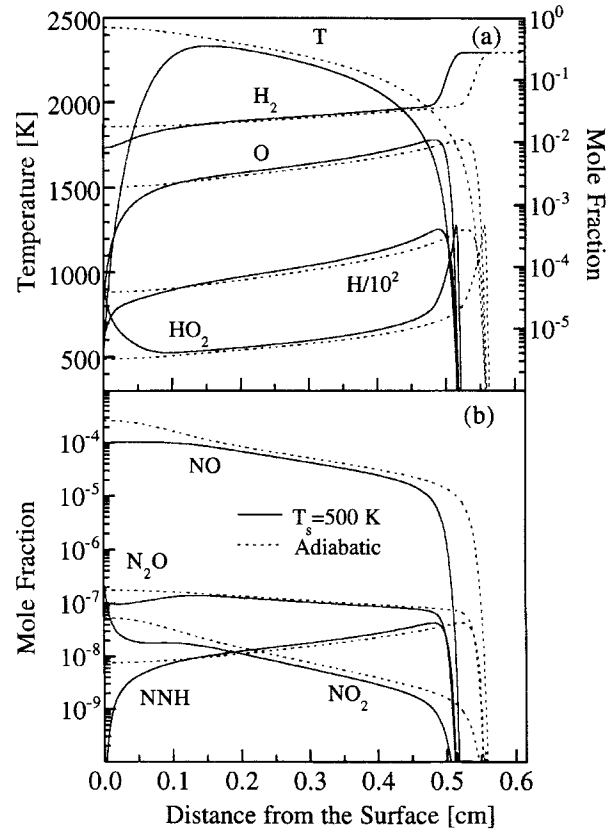

Figure 2. Profiles of temperature, fuel and selected radical species (panel a), and NNH and NO_x (panel b) at two surface temperatures for 28% inlet H_2/air.

This mixture exhibits a relatively thick thermal boundary layer. Reduction in surface temperature affects the species mole fractions only in a small sublayer of the thermal boundary layer. Thermal quenching slightly affects NO_x except of NO_2. The conditions are the same as in Figure 1.

Figure 2b shows the corresponding profiles of NNH and NO_x species. It is interesting to note that the reduction in surface temperature has little effect on NNH and NO_x away from the surface. On the other hand, close to the surface, it causes a small decrease only in the mole fractions of NO and N_2O, and a considerable increase in NO_2 and a drop in the mole fraction of NNH by two orders of magnitude. This behavior is remarkably different from the significant reduction of NO with decreasing temperature due to inlet composition for adiabatic flames shown in Figure 1b. This indicates that the surface temperature alone cannot explain NO_x emissions for this distributed system.

Figure 3a shows the net rates of production (if positive) or consumption (if negative) of selected species vs. the distance from the surface at the two surface temperatures chosen above. The adiabatic case is first analyzed. Close to the inlet, there is a peak in the production rate of NO with a corresponding trough in the consumption rate of N_2. Further downstream, these rates remain relatively constant. The rate of NNH production peaks closer to the inlet than that of NO, and becomes very low in the post-combustion zone.

The calculation and isolation of the contributions of various NO formation pathways has been discussed extensively in the literature. In particular, most studies have calculated the NO mole fraction with the full mechanism and compared this to the NO formed by eliminating one pathway at a time from the full mechanism (for example, Nicol et al., 1995). This procedure does not account for the competitive paths connecting the various pathways. Furthermore, while the direct contributions to NO are easily identifiable through the rates of specific reactions, there are indirect contributions to NO, particularly from NNH, through N and NH, that can become quite important at some conditions, and are difficult to quantify by this method. In particular, note that N can form by NNH and the thermal or Zeldovich path $N_2 + O \leftrightarrow NO + N$. We have found that this method produces reasonable results which, however, are not exactly additive.

We have constructed here a scheme that enables us to identify the net contribution of the three pathways, namely, the NNH, thermal, and N_2O one, to NO. First, reaction path analysis has been performed across the flame indicating that the intermediates N, NH, and HNO are in quasi-steady state, according to the chemical production ratio (Kalamatianos et al., 1998), except in the preheating zone of the flame very

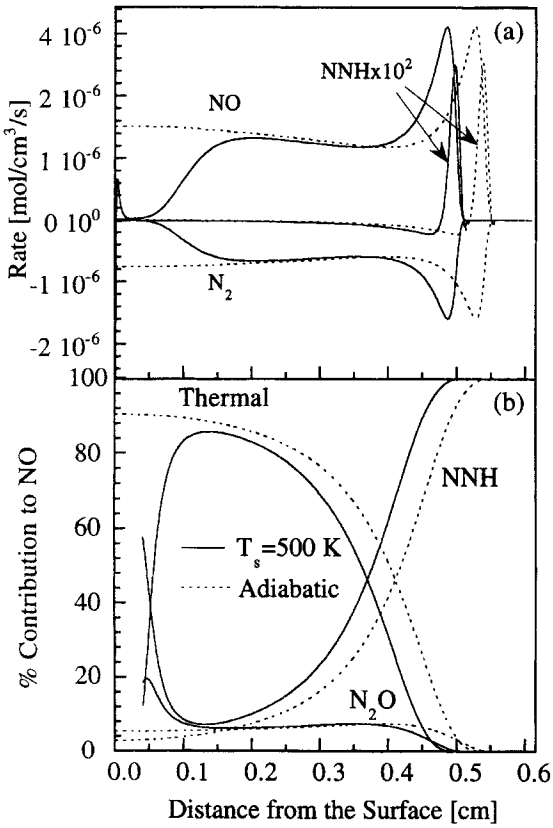

Figure 3. Rates of selected species (panel a) and percentage contribution of major NO production pathways (panel b) across the flame for 28% inlet H_2 in air at two surface temperatures.

In the post-combustion zone, the thermal pathway dominates in NO production, and the NNH pathway has an important contribution to NO near the inlet. The conditions are the same as in Figure 1.

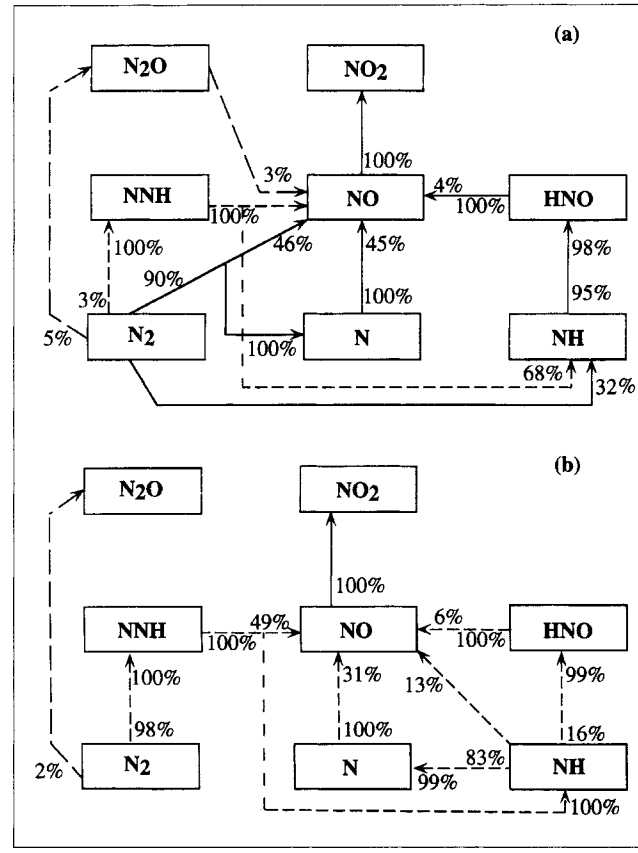

Figure 4. Reaction path analysis for the adiabatic case of the 28% inlet H_2 in air mixture, near the surface (panel a), and 0.52 cm away from the surface (panel b).

The conditions are the same as in Figure 1.

near the entrance. Consequently, their chemical rates of formation and consumption are equal. Thus, one can relate the rate of formation of NO from these species to the rate of consumption of major species such as NNH, N_2O, and N_2 to compute the indirect contributions to NO from the major pathways. This analysis indicates that the different contributions to NO production are as follows (the first term is the direct contribution, and the second the indirect one)

$$\text{thermal} = (-r_{58}) + (-r_{58})$$

$$\text{NNH} = (r_{49}) + (r_{49})$$

$$\text{N}_2\text{O} = (2r_{32} - r_{44}) + (-r_{44}),$$

where r_i refers to the rate of reaction i (mol·cm^{-3}·s^{-1}), and reaction numbers correspond to the ones in Table 2. The different paths are shown in Figure 4.

Figure 3b shows the net (direct plus indirect) percentage contribution of the different pathways to NO formation vs. the distance from the surface for the nonextinguishable mixtures. The NNH pathway dominates NO production near the inlet, becomes equally important to the thermal pathway ~ 1 mm downstream of the reaction zone, and is low near the surface compared to the Zeldovich mechanism. The N_2O pathway is not very important at these conditions. In the preheating zone of the flame, that is, at distances greater than 0.55 cm away from the surface, the quasi-steady-state hypothesis does not hold, and, hence, the contributions are not calculated. This is not of much concern since both the rate of NO production and the NO mole fraction are very low here.

In order to identify the specific reactions and species contributing to NO, a detailed reaction path analysis has been performed across the flame to complement the results of the lumped analysis shown above. Figure 4 shows some of the results obtained. Here, the arrows pointing towards a species refer to its production paths, while the arrows pointing away refer to consumption. If there are multiple reactions connecting two species (for example, R_{33}-R_{36} are involved in NO-NO_2 chemistry), only the net effect of these reactions is represented here. The numbers indicate the percentage contribution to the production or consumption of the species they are closest to.

The important initiation reactions for the various pathways are the thermal pathway (solid lines)

$$\text{N}_2 + \text{O} \leftrightarrow \text{NO} + \text{O} \quad R_{58}$$

the NNH pathway (short-dashed lines)

$$N_2 + H \leftrightarrow NNH \quad R_{65}$$

$$N_2 + H + M \leftrightarrow NNH + M \quad R_{66}$$

and the N_2O pathway (long-dashed lines)

$$N_2 + O + M \leftrightarrow N_2O + M. \quad R_{62}$$

Figure 4a shows the reaction path analysis for the NO_x species, at a distance of 0.004 cm away from the surface, at adiabatic conditions. NO is produced at 91% from the thermal pathway, partly from N_2 directly (R_{58}), and partly from the reaction

$$N + OH \leftrightarrow NO + H. \quad R_{31}$$

There is a small direct contribution from N_2O through the reaction

$$N_2O + H \leftrightarrow NO + NH \quad R_{44}$$

and an indirect one from NNH through NH and HNO. This is in agreement with Figure 3b, near the surface. NO is consumed at a very small rate to NO_2 in this case.

Figure 4b shows the reaction paths at a distance of ~ 0.52 cm away from the surface, corresponding to the peak in the NO production rate in Figure 3a. The thermal pathway is not contributing either to the production of NO or the consumption of N_2 in this case. The direct NNH pathway to NO

$$NNH + O \leftrightarrow NO + NH \quad R_{49}$$

has the maximum contribution to NO formation. The rest of the NO, arising from N, NH, and HNO, can also be traced back to NNH. Thus, at this position, the NNH pathway is dominant for NO production, in agreement with Figure 3b.

Now, we discuss the thermally quenched case of the nonextinguishable flame. Figure 3a shows also the rates of various species vs. the distance from the surface at a surface temperature of 500 K. While the boundary layer is slightly smaller than the adiabatic case, there is no perceptible change in the upstream peak in NO and NNH rates, and the trough in N_2 rate. On the other hand, close to the surface, the rate of consumption of N_2 approaches zero, and the rate of NO shows a nonmonotonic dependence, dropping near zero at ~ 0.06 cm away from the surface, increasing again closer to the surface to give a small production peak, and finally leading to consumption at the surface.

Figure 3b shows the corresponding percentage contribution of various pathways to NO production. Similar to the adiabatic case, near the inlet, the NNH pathway is important, and the contribution from the thermal pathway increases downstream. However, in this case, the thermal contribution goes through a maximum at ~ 0.1 cm away from the surface, and drops off rapidly close to the surface, due to the surface quenching leaving again the NNH pathway as the dominant one (see Figure 2a). The curves terminate abruptly near the surface, since N, NH, and HNO are no longer in quasi-steady state. However, the production rate of NO approaches zero, and eventually NO is consumed in this region, so analysis of the production pathways for NO is not important.

This behavior is interesting, because even when the surface is thermally quenched down to a low temperature, there is considerable NO throughout the boundary layer, as seen in Figure 2b. The large mole fraction of NO near the surface has been attributed to convective transport from the upstream regions of high production.

Detailed reaction path analysis for the quenched, nonextinguishable mixture has revealed that the pathways upstream are the same as in the adiabatic case. The consumption of NO close to the surface in this case has been found to lead to increased NO_2, through the low activation path

$$NO + HO_2 \leftrightarrow NO_2 + OH. \quad R_{33}$$

Thus, nonextinguishable flames exhibit high temperatures and high rates of species production over the bulk of the boundary layer, irrespective of the surface temperature. Surface thermal quenching does not affect the chemistry upstream and only results in slowing down of the rates closer to the surface, accompanied by some interesting NO_x interconversions. From a practical point of view, one needs to increase the coupling between the flame and the surface to reduce NO_x emissions by thermal quenching. Methods to achieve that are described next.

Extinguishable flames

Figure 5a shows the profiles of temperature and mole fractions of selected species for a 10% inlet H_2/air mixture at different surface temperatures, viz., 1,450 K (adiabatic temperature) and 1,199 K (close to extinction). Such flames are thin compared to the nonextinguishable one discussed above, and are stabilized at or near the surface, depending on the surface temperature. In contrast to strong, nonextinguishable flames discussed above, the thermal interaction between the flame and a surface is now strong due to the proximity of the flame to the surface. When the surface temperature decreases, the flame becomes substantially thinner and approaches the surface until it collapses at extinction due to small concentrations of active radicals.

Figure 5b shows the corresponding profiles of NNH and NO_x species at these conditions. Since there is no production of NO_x away from the surface, the NO_x levels drop dramatically throughout the flame, as the temperature decreases. The mole fraction of NNH is also seen to decrease as the surface temperature decreases. The rate of production of NO has been found to be substantially lower, compared to the nonextinguishable flame. The NNH pathway is the dominant one throughout the flame, as the temperatures are too low for the thermal one to have significant contribution. It appears then that the fuel composition strongly affects the flame location and its coupling with the surface, and provides one method to control NO_x emissions by operating sufficiently fuel-lean while thermally quenching the surface (such as using a high emissivity material).

Role of Strain Rate in Emissions

The main qualitative features of the system described above have been found to be generic over a wide range of strain rates examined, between 10^2 s^{-1} and 10^4 s^{-1}, and are determined by the bifurcation behavior of a mixture. Thus, for ex-

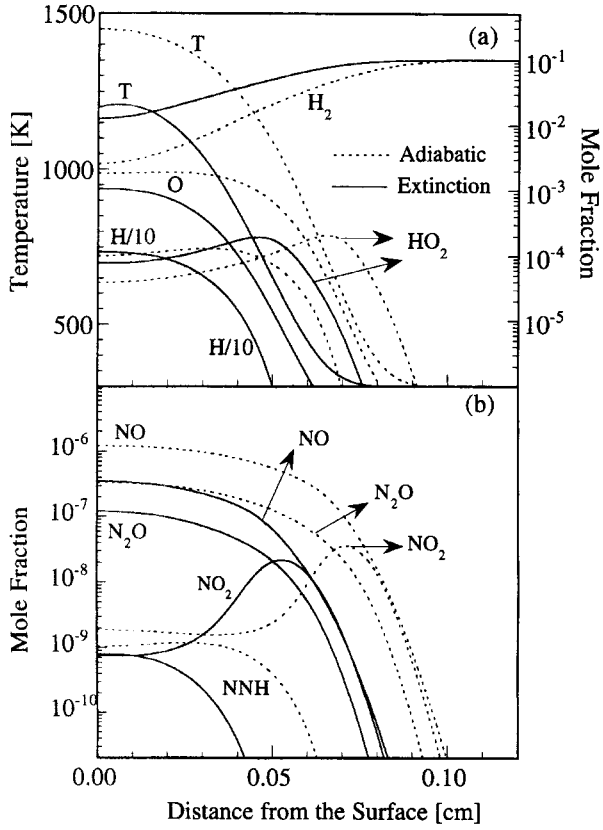

Figure 5. Profiles of temperature, fuel, and selected radicals (panel a), and NNH and NO_x species (panel b) for a 10% inlet H_2/air mixture at adiabatic and extinction conditions.

This flame is thin and stabilized at or near the surface. The thermal coupling between the flame and the surface is strong, and surface quenching significantly reduces NO_x with a concomitant rise in unburned fuel. The conditions are the same as in Figure 1.

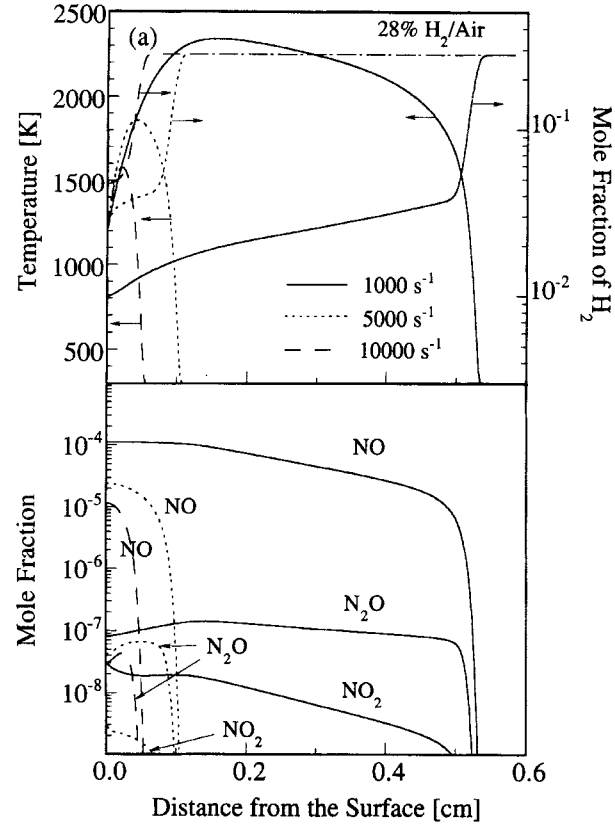

Figure 6. Profiles of temperature and fuel (panel a) and NO_x (panel b) at a surface temperature of 1,200 K at various strain rates for 28% inlet H_2/air.

An increase in strain rate pushes the flame closer to the surface and enhances the surface–flame thermal coupling, while reducing NO_x. The conditions are a pressure of 1 atm and an inlet temperature of 25°C.

tinguishable mixtures, the thermal coupling between the surface and the gas phase is very important in determining the fuel and NO_x emissions. On the other hand, for nonextinguishable flames, the emissions are not much influenced by the temperature of the surface.

The strain rate strongly affects the flame-surface coupling and provides, in conjunction with thermal quenching, another method to control NO_x emissions. For all mixtures, increasing the strain rate leads to an approach of the flame toward the surface which in turn results in stronger coupling between the surface and the flame, and a reduction of both the autothermal and the nonextinction regimes. Figure 6 shows, as an example, the fuel, temperature, and NO_x profiles at a surface temperature of 1,200 K for 28% inlet H_2 in air. An increase in the strain rate pushes the flame closer to the surface, and the thickness of the thermal boundary layer considerably decreases. Hence, temperatures in the bulk of the boundary layer and the overall reactivity of the system are reduced, resulting in higher mole fractions of the fuel near the surface and lower NO_x emissions, as shown in Figure 6b. Analysis of the pathways for NO production shows that the NNH pathway becomes the dominant one at high strain rates, over the whole boundary layer, due to the lower temperatures. In addition, the temperature gradient increases near the surface as indicated in Figure 6a, representative of stronger thermal coupling between the flame and the surface.

While the results presented in Figure 6 are for nonextinguishable mixtures, similar trends also hold for the lean, extinguishable mixtures, such as 10% H_2 in air. However, the increased thermal coupling between the surface and the flame at the higher strain rates also has an important influence on the extinguishability of the system, resulting in extinction at higher surface temperatures. In general, an increase in the strain rate at a fixed surface temperature leads to a decrease in NO_x emissions, accompanied by a rise in fuel emissions at sufficiently high strain rates examined here. To achieve reduction in NO_x emissions in radiant combustors, these simulations indicate that sufficiently fast flows and/or fuel-lean mixtures are needed to provide strong surface-flame thermal coupling. Obviously, under such conditions the possibility for extinction is enhanced.

Role of Wall Radical Quenching in Emissions

The above simulations assumed an inert surface. Recombination of radicals on cold walls was proposed many years ago

Table 3. Surface Reaction Mechanism Considered for Each Species

Species removed	Reactions	Sticking coefficient or pre-exponential (s^{-1})
H	$H + * \rightarrow H*$	1.0
	$2H* \rightarrow H_2 + 2*$	10^{13}
O	$O + * \rightarrow O*$	1.0
	$2O* \rightarrow O_2 + 2*$	10^{13}
OH	$OH + * \rightarrow OH*$	1.0
	$2OH* \rightarrow H_2O + O* + *$	10^{13}
	$2O* \rightarrow O_2 + 2*$	10^{13}
HO_2	$HO_2 + 2* \rightarrow OH* + O*$	1.0
	$2OH* \rightarrow H_2O + O* + *$	10^{13}
	$2O* \rightarrow O_2 + 2*$	10^{13}

The activation energy of all steps has been taken equal to zero.

to explain ignition data in vessels with various coatings (Lewis and von Elbe, 1987; Dixon-Lewis and Williams, 1977; Gray and Scott, 1990). Here, to understand the effect of the loss of radicals on emissions, due to radical wall recombination reactions, simulations were performed for the first time by incorporating an adsorption-surface reaction-stable species desorption mechanism for selected radicals. A radical adsorbs onto the surface at a rate proportional to its sticking coefficient and its partial pressure above the surface, based on kinetic theory of ideal gases (Bui et al., 1997). The adsorbed radicals recombine on the surface to form stable species, which then desorb into the gas phase. Thus, the net effect of this chemical interaction between the gas phase and the surface is to replace the radicals in the gas phase with stable species while properly conserving mass. As an example, the chemistry steps included for H are

$$H_{gas} \rightarrow H_{surface} \rightarrow \frac{1}{2} H_{2\,gas} \quad S_1$$

and similar reaction sequences were included for the other radicals as well, as shown in Table 3.

The sticking coefficient for each radical adsorption was chosen to be 1.0, and the recombination process was assumed to be nonactivated. The pre-exponential of each recombination reaction was estimated based on transition state theory (Waugh, 1996). This set of parameters provides radical quenching at the highest possible rate, as determined by the mass-transfer rate to the surface independently of details of the surface reaction mechanism which are still unknown. It thus provides an estimate on the maximum influence of radical recombination on emissions. Such a reaction mechanism has been recently employed to study the effect of radical wall recombination on the stability and flammability of H_2/air flames (Aghalayam and Vlachos, 1998).

Figures 7a and 7b show the fuel and NO_x mole fractions adjacent to the surface, as a function of the surface temperature for 28% and 10% inlet H_2 in air, respectively, for three cases: the nominal inert surface, a surface quenching out H radicals, and a surface quenching out all radicals simultaneously. The effect of quenching out one radical at a time has been studied to isolate the relative importance. H and OH radicals have been found to be the most important, whereas

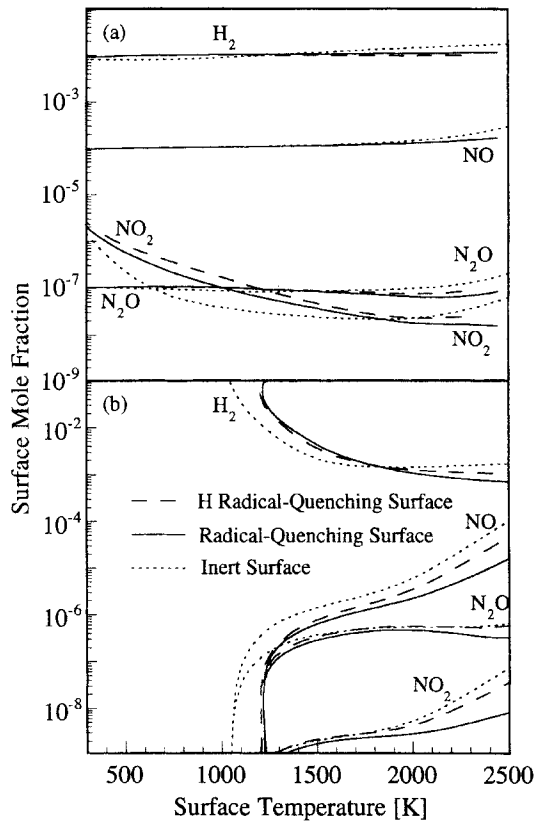

Figure 7. Surface mole fraction of fuel and NO_x when all radicals are quenched at the surface for 28% H_2 in air (panel a) and 10% H_2 in air (panel b), as compared to the corresponding inert surface and H radical quenching surface cases.

For the nonextinguishable flame, H radical quenching increases NO_2 at low surface temperatures. For extinguishable flames, radical quenching affects emissions primarily near extinction. The conditions are the same as in Figure 1.

O and HO_2 radicals do not lead to significant changes in the emissions. For the sake of clarity, only the above mentioned three cases are plotted.

For nonextinguishable mixtures, there is a small influence from radical recombination on emissions, that is, the flame-surface chemical coupling is also weak. The most noticeable feature is a significant increase (up to an order of magnitude) in NO_2 near the surface. Reaction path analysis has shown that this increase in NO_2 is due to a retardation of reaction R_{36}, $NO_2 + H \leftrightarrow NO + OH$, which converts NO_2 to NO, caused by a surface loss of H radicals.

For extinguishable mixtures, at relatively high surface temperatures, removal of H radicals can result in lower NO_x emissions, as compared to an inert surface (a reduction by a factor of two in NO) with a concomitant increase in fuel mole fractions (by a factor of three) due to desorption of H_2 by reaction S_1 and retardation of homogeneous combustion near the surface due to loss of H. A comparable effect is found when OH radicals are quenched out, whereas the effect of quenching out O and HO_2 radicals is less pronounced. The effect of quenching out simultaneously all radicals according

to reactions listed in Table 3 is to reduce the NO and NO_2 near the surface by up to an order of magnitude, with a corresponding increase in fuel emissions.

We should note that when radicals are quenched out, there is some influence on the ignition and extinction temperatures, as compared to an inert surface. This effect is especially prominent for the quenching out of H radicals, as first suggested some years ago assuming the surface as an infinitely fast sink of specific radicals (Vlachos et al., 1993). As a result, NO_x concentrations near extinction are more strongly affected by radical wall recombination.

Our results here indicate that even though radical wall recombination may affect quantitatively NO_x concentrations, the overall effects for surface-stabilized flames are not dramatic, except near extinction where flame–surface interactions are strong. Inert surfaces may then serve as an important case for estimation of emissions, especially since details of the wall chemistry change with material and temperature in a poorly understood way.

Conclusions

The production and destruction of NO_x and H_2 have been studied in the combustion of premixed H_2/air mixtures impinging on a flat, inert surface, using detailed gas-phase chemistry and multicomponent transport. For adiabatic flames, NO_x emissions decrease considerably with a decrease in inlet H_2 composition, due to the combined effect of the flame approaching the surface and a reduction in the maximum adiabatic temperature.

For nonextinguishable flames, the thermal coupling between a flame and a surface is relatively weak. As a result, thermal quenching of the surface has little influence on the gas-phase chemistry, except in a small sublayer near the surface. These flames are stabilized away from the surface, and NO is mainly produced in the bulk and convected to the surface. An interesting deviation from this behavior is NO_2 in the frozen sublayer, which increases due to the reaction R_{33}, $NO + HO_2 \leftrightarrow NO_2 + OH$. Weak, extinguishable flames are stabilized at or near the surface, and hence, the thermal coupling between the gas phase and a surface is strong. Thermal quenching of the surface considerably decreases NO_x emissions but at the expense of increased H_2 emissions. The influence of surface thermal quenching on NO_x depends on the thickness of the thermal boundary layer, which is determined mainly by the strain rate and the inlet composition. Thin flames show strong coupling with the surface, and lead to lower NO_x.

Quenching of radicals at the stagnation surface has overall small influence on emissions of nonextinguishable mixtures, except of an increase in NO_2 near the surface due to a slowing down of the reaction R_{36}, $NO_2 + H \leftrightarrow NO + OH$. The effect of radical quenching on emissions is, however, stronger near extinction, leading to a lower NO mole fraction. Increasing the strain rate was found to enhance the flame–surface coupling and reduce NO_x emissions. These simulations indicate that to reduce NO_x by thermal and radical quenching, sufficiently fuel-lean mixtures or thin boundary layers (fast flows) are desirable.

The important pathways for NO production in H_2/air flames vary considerably with the conditions of operation. The thermal or Zeldovich mechanism is very important at high temperatures in the post-combustion zone, while the NNH mechanism acquires importance for extinguishable flames at all conditions, and for nonextinguishable flames in the low-temperature regions near the inlet or a thermally quenched surface.

Acknowledgments

Acknowledgment for partial support of this work is made to the Office of Naval Research with Dr. G. D. Roy through a Young Investigator Award under contract number N00014-96-1-0786.

Notation

D_j = multicomponent diffusion coefficient of species j in mixture
k = thermal conductivity, cal cm^{-1} K^{-1} s^{-1}
k_0 = reaction pre-exponential, mol, cm, s^{-1}
m_g = number of gas-phase species not including the carrier gas
m_s = number of surface species
M_j = molecular weight of jth species, g/gmol
$\bar{M}$ = average molecular weight of the gas mixture, g/gmol
N_s = number of surface reactions
P_w = power input per unit area, cal cm^{-2} s^{-1}
r_i^s = rate of ith surface reaction, mol cm^{-2} s^{-1}
T = temperature, K
W_j = weight fraction of species j
y = spatial coordinate

Greek letters

β = exponent on temperature in the reaction rate expression
θ_j = coverage of species j on the surface
ρ = density of the mixture, g cm^{-3}
ν_{ij} = stoichiometric coefficient of jth species in ith reaction
ΔH_i^s = heat of ith surface reaction, Kcal mol^{-1}
$\omega_i(j)$ = third-body collisional efficiency of species j in reaction i

Superscripts and subscripts

e = entrance of the reactor
g = gas
i = reaction
j = species
s = surface
$*$ = vacancies/adsorbed species

Literature Cited

Aghalayam, P., and D. G. Vlachos, "The Role of Radical Wall Quenching in Flame Stability and Wall Heat Flux: Hydrogen/Air Mixtures," *Combust. Theory and Modelling*, in press (1998).

Bowman, C. T., R. K. Hanson, D. F. Davidson, W. C. Gardiner Jr., V. Lissianski, G. P. Smith, D. M. Golden, M. Frenklach, and M. E. Goldenberg, available from http: //www.me.berkeley.edu/gri_mech/ (1995).

Bui, P.-A., D. G. Vlachos, and P. R. Westmoreland, "Modeling Ignition of Catalytic Reactors with Detailed Surface Kinetics and Transport: Combustion of H_2/Air Mixtures over Platinum Surfaces," *Ind. Eng. Chem. Res.*, **36**, 2558 (1997).

Daniel, W. A., "Flame Quenching at the Walls of an Internal Combustion Engine," *Sixth Symp. (Int.) on Combustion/The Combustion Inst.*, 886 (1956).

Dixon-Lewis, G., and D. J. Williams, "The Oxidation of Hydrogen and Carbon Monoxide," *Comprehensive Chemical Kinetics*, C. H. Bamford and C. F. H. Tipper, eds., Elsevier, Amsterdam, p. 1 (1977).

Gray, P., and S. K. Scott, *Chemical Oscillations and Instabilities, Nonlinear Chemical Kinetics*, Clarendon Press, Oxford (1990).

Hocks, W., N. Peters, and G. Adomeit, "Flame Quenching in Front of a Cold Wall under Two Step Kinetics," *Combustion and Flame*, **41**, 157 (1981).

Hori, M., "Experimental Study of Nitrogen Dioxide Formation in Combustion Systems," *Twenty-First Symp. (Int.) on Combustion/The Combustion Inst.*, 1181 (1986).
Hori, M., "Nitrogen Dioxide Formation by the Mixing of Hot Combustion Gas with Cold Air," *Twenty-Second Symp. (Int.) on Combustion/The Combustion Inst.*, 1175 (1988).
Hori, M., N. Matsunaga, P. C. Malte, and N. M. Marinov, "The Effect of Low-Concentration Fuels on the Conversion of Nitric Oxide to Nitrogen Dioxide," *Twenty-Fourth Symp. (Int). on Combust./Combust. Inst.*, 909 (1992).
Kalamatianos, S., Y. K. Park, and D. G. Vlachos, "Two-Parameter Continuation Algorithms for Sensitivity Analysis, Parametric Dependence, Reduced Mechanisms, and Stability Criteria of Ignition and Extinction," *Combust. Flame*, **112**, 45 (1998).
Kee, R. J., G. Dixon-Lewis, J. Warnatz, M. E. Coltrin, and J. A. Miller, "A FORTRAN Computer Code Package for the Evaluation of Gas-Phase Multicomponent Transport Properties," Sandia National Laboratories Report, SAND86-8246 (1990).
Kiehne, T. M., R. D. Matthews, and D. E. Wilson, "The Significance of Intermediate Hydrocarbons During Wall Quench of Propane Flames," *Twenty-First Symp. (Int) on Combustion/Combust. Inst.*, 481 (1986).
Lewis, B., and G. von Elbe, "Chemistry and Kinetics of the Reactions between Gaseous Fuel and Oxidants," in *Combustion, Flames and Explosions of Gases*, Academic Press, Orlando, p. 1 (1987).
Nicol, D. G., R. C. Steele, N. M. Marinov, and P. C. Malte, "The Importance of the Nitrous Oxide Pathway to NO_x in Lean-Premixed Combustion," *Trans. ASME*, **117**, 100 (1995).
Sano, T., "NO_2 Formation in the Mixing Region of Hot Burned Gas with Cool Air," *Comb. Sci. and Technol.*, **38**, 129 (1984).
Sano, T.,"NO_2 Formation in the Mixing Region of Hot Burned Gas with Cool Air—Effect of Surrounding Air," *Combust. Sci. and Tech.*, **43**, 259 (1985).
Sloane, T. M., and A. Y. Schoene, "Computational Studies of End-Wall Flame Quenching at Low Pressure: The Effects of Heterogeneous Radical Recombination and Crevices," *Combust. and Flame*, **49**, 109 (1983).
Vlachos, D. G., "The Interplay of Transport, Kinetics, and Thermal Interactions in the Stability of Premixed Hydrogen/Air Flames near Surfaces," *Combust. Flame*, **103** (1-2), 59 (1995).
Vlachos, D. G., P.-A. Bui, Y. K. Park, and P. Aghalayam, "Numerical Bifurcation Theory Applied to Real Chemistry, Premixed Flames: Flame Stability and Pollution Abatement," in *Advanced Computation and Analysis of Combustion*, G. D. Roy, S. M. Frolov, and P. Givi, eds., ENAS Publishers, Moscow, p. 100 (1997).
Vlachos, D. G., L. D. Schmidt, and R. Aris, "Ignition and Extinction of Flames near Surfaces: Combustion of H_2 in Air," *Combustion and Flame*, **95**, 313 (1993).
Vlachos, D. G., L. D. Schmidt, and R. Aris, "Ignition and Extinction of Flames near Surfaces: Combustion of CH_4 in Air," *AIChE J.*, **40**(6), 1005 (1994).
Waugh, K. C., "Kinetic Modelling of Industrial Catalytic Processes based upon Fundamental Elementary Kinetics under Ultra high Vacuum," *Chem. Eng. Sci.*, **51**, 1533 (1996).
Westbrook, C. K., A. A. Adamczyk, and G. A. Lavoie, "A Numerical Study of Laminar Flame Wall Quenching," *Combust. Flame*, **40**, 81 (1981).
Williams, A., R. Woolley, and M. Lawes, "The Formation of NO_x in Surface Burners," *Combust. Flame*, **89**, 157 (1992).

Manuscript received Mar. 11, 1998, and revision received July 8, 1998.